Measuring matter effects in Neutron star - Black hole binaries with Advanced LIGO

People across the Atlantic
(Dated: November 10, 2015)

Abstract

I. INTRODUCTION

The Advanced LIGO (aLIGO) observatories began their first observing run "O1" in September, 2015. With both detectors a factor of $3-4$ more sensitive than their first-generation counterparts, we have access to ≈ 50 times more spacial volume of the universe at every instant. Within a 3 month observing run, these detectors would have access to as many binary mergers as initial-LIGO detectors did in ~ 6 years of coincident operation. Through gradual updates, both of these instruments will reach their design sensitivity by 2019, at which point they will like detect around 70 binary mergers a year [1].

Coalescing binaries containing a neutron star (NS) and a black hole (BH) are one of the most important sources of gravitational waves (GW) with the aLIGO and Virgo instruments, which expect to detect $\mathcal{O}(10)$ of such systems every year [1]. Conventional astronomical methods have, to date, made observations of NSs with masses between $XX - YYM_\odot$ and spin $|\vec{\chi} \lesssim 0.05$. On the other hand, indirect observations of BHs have placed the masses of stellar-collapse BHs between $5-35M_\odot$, with spin angular momenta ranging from low to nearly extremal values (i.e., nearly as fast as possible - see, e.g. [2–4] for examples of nearly extremal estimates of BH spins, and see Refs. [5, 6] for recent reviews of astrophysical BH spin measurements). [Do we want to emphasize on BH spins here?].

One question that aLIGO is likely to probe is 'what is the nature of matter at nuclear densities', i.e. what is the equation of state (EoS) of neutron stars. The EoS determines the compactness of NSs, which determines how early in the coalescence will the NS be tidally disrupted by the gravitational field of the BH, resulting in the formation of an accretion disk and/or ejection of unbound matter. This makes NSBH mergers are one of the prime targets of the program for joint detection of GW and electromagnetic signals. The difficulty in discerning the matter effects in an NSBH merger GW signal lies in distinguishing it reliably from a BHBH merger signal. The earlier the NS disrupts, the more orbits there are over which the effect of NS disruption is visible. Where exactly does disruption happen is governed both by the mass-ratio of the binary, as well as the spin on the BH. Larger BHs (with $q = m_{\rm BH}/m_{\rm NS} \gtrsim 7$), as well as BHs with large retrograde spins ($\chi_{\rm BH} \lesssim 0$), tend to swallow the NS whole due to a rapid merger (i.e. without it disrupting before the inner-most stable circular orbit (ISCO) is reached). On the other hand, binaries with mass-ratios $q = 2-5$ with large pro-grade $\chi_{\rm BH}$ can disrupt much before merger, leaving their imprint in the GW signal emitted close to $1.7-2$ kHz.

The goal of this paper is to probe the distinguishability of BHBH and NSBH mergers, focusing at the effects of the BH mass, BH spin, and NS tidal deformability. We also investigate the accuracy with which aLIGO can measure the tidal deformability parameter $\Lambda_{\rm NS} \sim (R/M)^5_{\rm NS}$. For both of these studies, we will use the zero-detuning high-power noise curve for the aLIGO detectors. In addition, we also study the effect of tuning aLIGO over a narrow frequency range aimed at NSBH mergers. We use the models published in Ref. [7, 8] to simulate NSBH merger waveforms.

Current status:

Below we explain the outline the different calculations performed in this paper:

1. We choose the following values of different NSBH binary parameters:
   (a) $m_{\rm NS} = 1.35M_\odot$;
   (b) $q = m_{\rm BH}/{\rm NS} = \{2, 3\}$;
   (c) $\chi_{\rm NS} = 0$;
   (d) $\chi_{\rm BH} = \{-0.5, 0, +0.5\}$;
   (e) $\Lambda = \{500, 1000, 2000\}$ ($\Lambda = 0 \implies$ BHBH).
2. For each system, corresponding to one of all possible unique combinations of the above parameter choices, we carry out three parameter estimation tests:
   (a) BH-BH signals injected, recovered with BH-BH waveforms (control),
   (b) NS-BH signals injected, recovered with BH-BH waveforms, (current approach) and
   (c) NS-BH signals injected, recovered with NS-BH waveforms.

   Injections were made at different SNR values:
   (a) $\rho = \{20, 30, 50, 70, 90, 120\}$.

   Choice of emcee parameters:
   (a) $N_{\rm samples} = 150,000$;
   (b) $N_{\rm walkers} = 100$;
   (c) $N_{\rm burn-in} = 500$;

and choice of prior boundaries:

(a) $m_{\rm BH} \in [1.2, 25] M_\odot$;

(b) $m_{\rm NS} \in [1.2, 15] M_\odot$;

(c) $\Lambda \leq 4000$;

(d) $\sigma(\Lambda) = 100$ (for chains where templates are NS-BH waveforms).

3. Results are shown in Fig. 1- 8.

II. TECHNIQUES

A. Modeling tidal deformation during inspiral

Describe the PN terms used here

B. Modeling tidal disruption near merger

Describe the Lackey et al model

C. MCMC methods

Describe the emcee-based PE code

III. HOW ARE DETECTION SEARCHES AFFECTED BY NOT INCLUDING NS MATTER EFFECTS

See what is the loss in SNR if we recover NSBH signals with a template bank of BH-BH waveforms? It is very likely that the answer would be: $< 1\%$. But it is very interesting to show that for spinning BHs!

IV. HOW IS PE AFFECTED BY NOT INCLUDING NS MATTER EFFECTS?

Advanced LIGO searches and parameter estimation efforts aimed at binaries containing NS and stellar-mass BHs are poised to use waveform models that do not include the effects of the NS tidal deformability [9]. While this is not expected to be the dominant source of error at low SNRs, it will likely introduce a systematic bias in the physical parameters that we recover from GW observations. In this section, we study the impact of the same for binaries where the BH spins are aligned to the orbital angular momentum.

1. Above what SNR values, below what mass-ratios, above what BH spins, etc, do we begin to care about NS deformability?
"one interesting plot to make would be the parameter bias (max-Likelihood parameters minus true parameters) vs SNR, as functionals of q/sBH/Lambda, when using T signals recovered with N templates."
" another interesting plot to make would be the fitting-factors recovered with a discrete (search oriented) template bank of BBH waveforms, for NSBH signals of loudness, deformability, spins, mass-ratios, etc. Which parameter plays the dominant role in paramter regions where the bank does not suffice to recover the desired threshold of optimal SNR?"

Could have subsections for different frequency-optimized aLIGO noise curves ?

V. WHAT DO WE GAIN BY USING TEMPLATES THAT INCLUDE NS MATTER EFFECTS?

Having shown in the previous section that we begin to care for NS tidal effects for signals in the XXX corner of the paraemter space, with SNRs above YY, here we investigate the effect of the improvement in the accuracy of the recovered parameters when tidal effects are included in the templates.

1. What is the reduction in the bias of the maximum likelihood parameters when using tidal templates?
"Plot the ratio of the bias between N templates and T templates (against T signals), as a function of SNR."

2. What is the reduction in the uncertainty in binary mass and spin, if any?
"show how the the 90% confidence intervals shrink, as a function of SNR, when we go from using N templates to T templates."

Could have subsections for aLIGO and ET ?

VI. DISCUSSION

Discussion

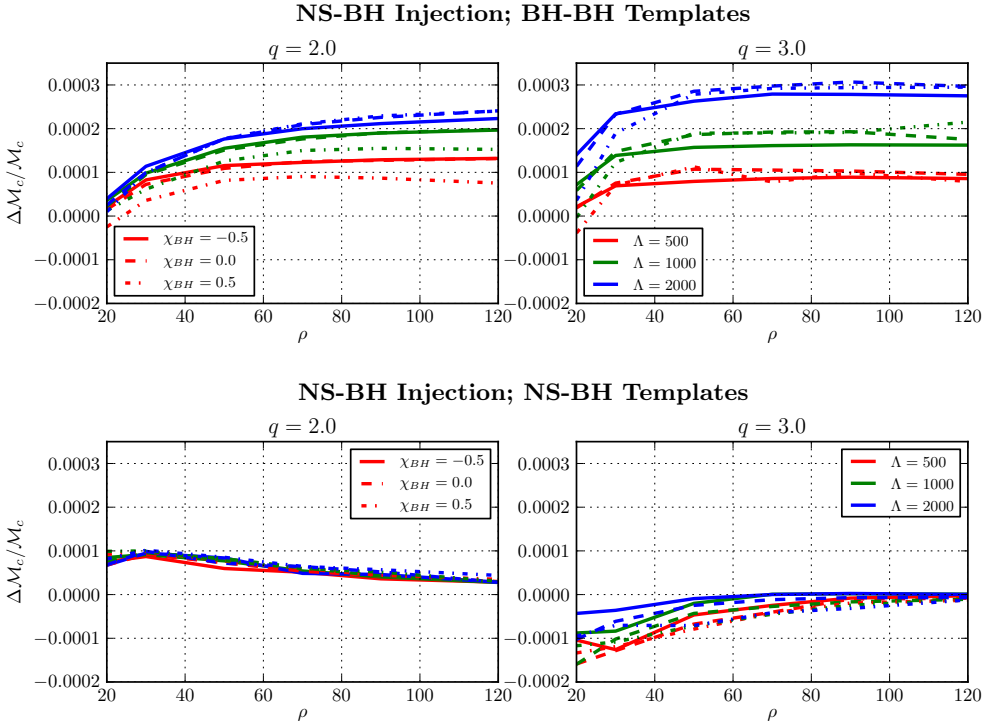

FIG. 1. These figures show the (fractional) difference between the chirp mass value corresponding to the median of its posterior probability distribution, and the actual injected chirp mass, as a function of the signal-to-noise-ratio (SNR) of the injected signal. In the top row, NS matter effects (inspiral and merger) are included in the injections but not in templates. This corresponds to the current plan for aLIGO parameter estimation studies. The bottom row shows the effect of additionally including NS matter effects in the templates. In each row, the left and right panel correspond to $q = m_{\rm BH}/m_{\rm NS} = \{2, 3\}$, respectively. In each panel, the color of each curve corresponds to the value of NS deformability parameter ($\Lambda = \{500, 1000, 2000\}$), and line-style corresponds to the value of the dimensionless spin on the BH ($\chi_{\rm BH} = \{-0.5, 0, +0.5\}$).

ACKNOWLEDGMENTS

Acknowledgments

REFERENCES

[1] J. Abadie, B. P. Abbott, R. Abbott, M. Abernathy, T. Accadia, F. Acernese, C. Adams, R. Adhikari, P. Ajith, B. Allen, and et al., Classical and Quantum Gravity **27**, 173001 (2010), arXiv:1003.2480 [astro-ph.HE].

[2] J. E. McClintock, R. Shafee, R. Narayan, R. A. Remillard, S. W. Davis, and L.-X. Li, Astrophys. J. **652**, 518 (2006).

[3] J. Miller, C. Reynolds, A. Fabian, G. Miniutti, and L. Gallo, Astrophys.J. **697**, 900 (2009), arXiv:0902.2840 [astro-ph.HE].

[4] L. Gou, J. E. McClintock, R. A. Remillard, J. F. Steiner, M. J. Reid, *et al.*, Astrophys.J. **790**, 29 (2014).

[5] J. E. McClintock, R. Narayan, and J. F. Steiner, Space Sci.Rev. **183**, 295 (2014), arXiv:1303.1583 [astro-ph.HE].

[6] C. S. Reynolds, Space Science Reviews **183**, 277 (2014), arXiv:1302.3260 [astro-ph.HE].

[7] B. D. Lackey, K. Kyutoku, M. Shibata, P. R. Brady, and J. L. Friedman, Phys. Rev. D **89**, 043009 (2014), arXiv:1303.6298 [gr-qc].

[8] F. Pannarale, E. Berti, K. Kyutoku, B. D. Lackey, and M. Shibata, Phys. Rev. **D92**, 084050 (2015), arXiv:1509.00512 [gr-qc].

[9] T. D. Canton, A. H. Nitz, A. P. Lundgren, A. B. Nielsen, D. A. Brown, *et al.*, (2014), arXiv:1405.6731 [gr-qc].

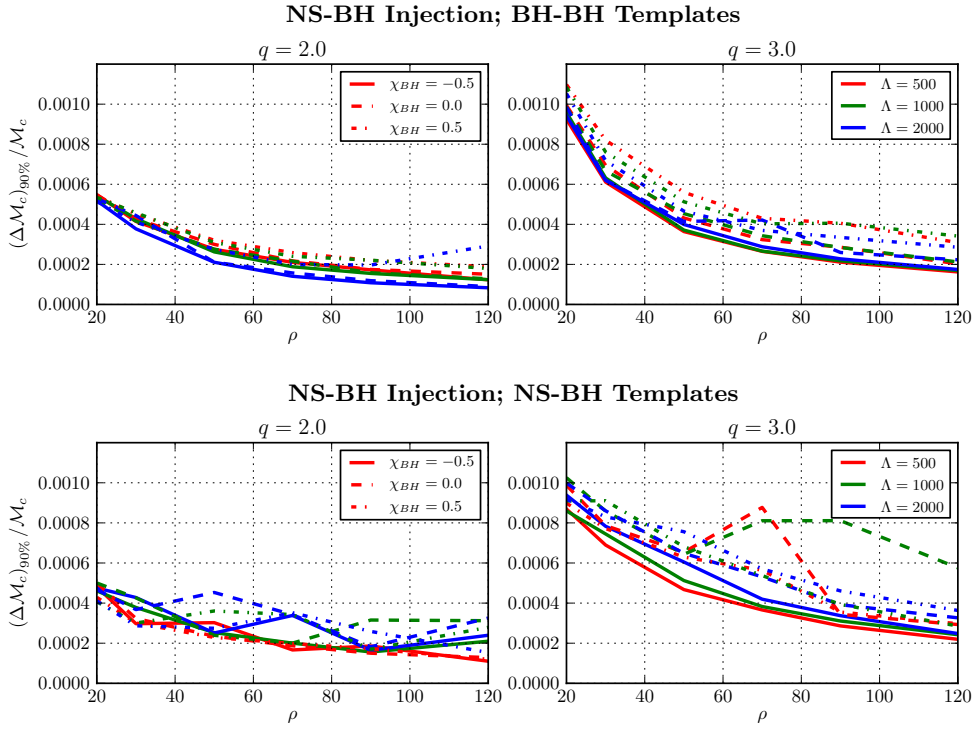

FIG. 2. These figures are similar to Fig. 1 with the difference that here we show the width of the 90% confidence interval (recovered) for chirp mass, as a function of the injected SNR. Note that the confidence interval's width is normalized by the injected parameter value.

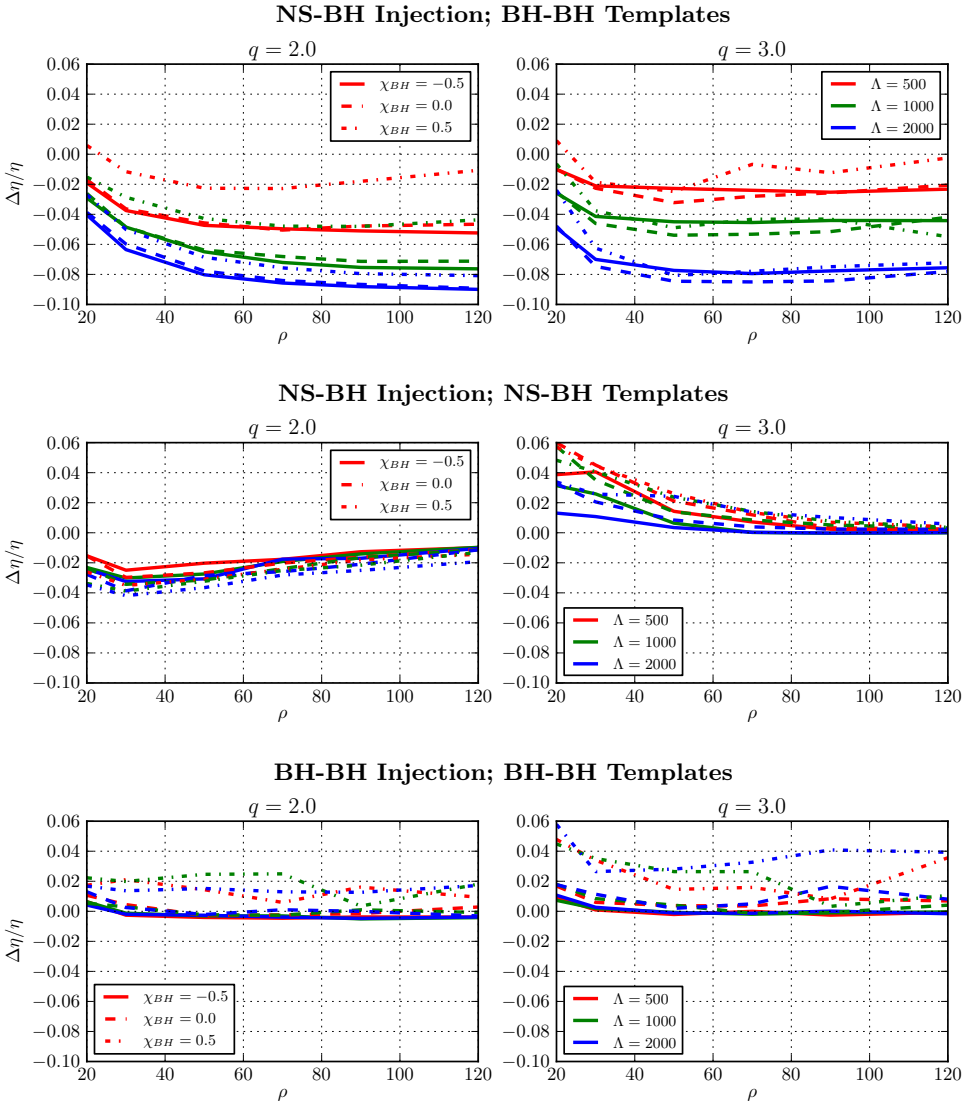

FIG. 3. This figure (top two rows) is similar to Fig. 1, with the difference that we consider the systematic bias in the dimensionless mass-ratio η here. In the bottom row we show control runs where both signal and template waveforms lack matter effects.

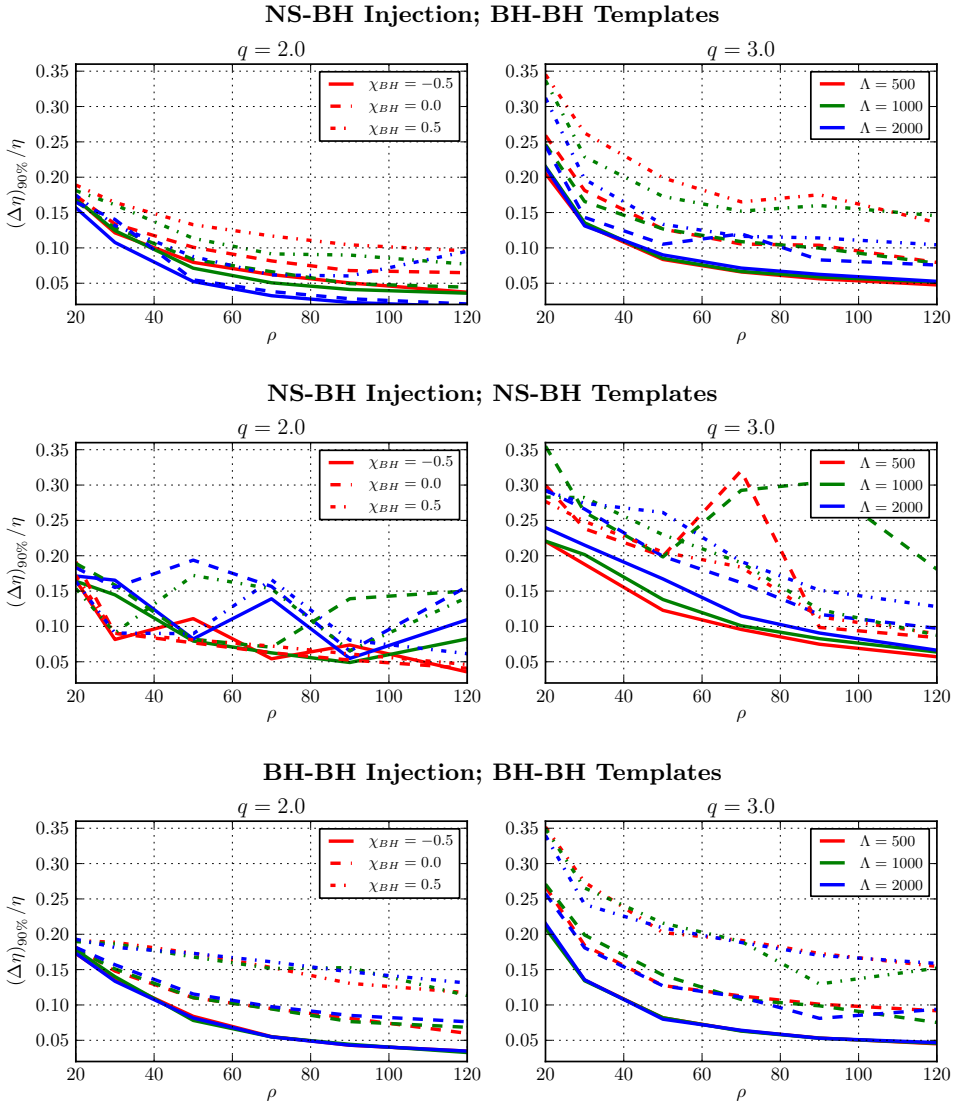

FIG. 4. This figure (top two rows) is similar to Fig. 2, with the difference that we consider the confidence intervals in the recovery of the dimensionless mass-ratio η here. The bottom row here is similar to Fig. 3 with the difference that width of the 90% confidence interval is shown here.

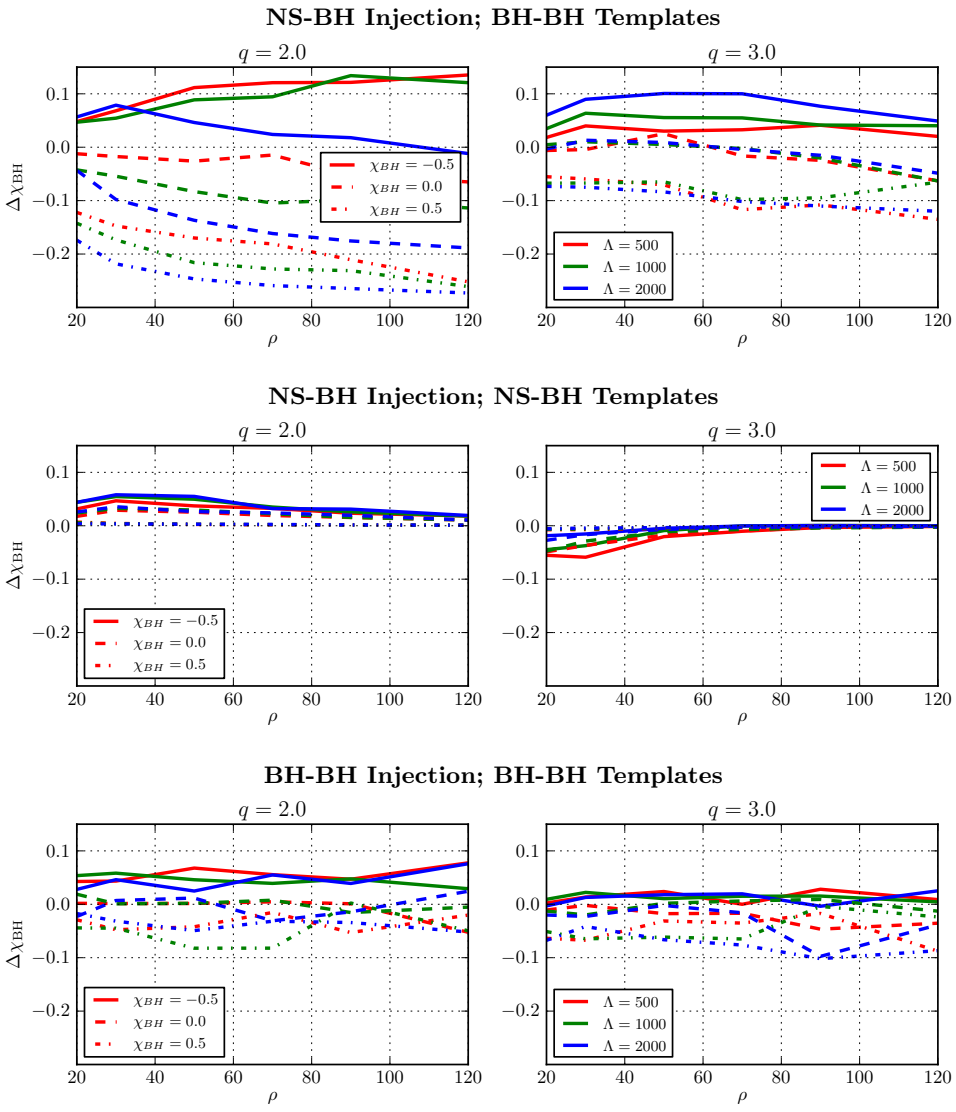

FIG. 5. The top two rows in this figure are similar to Fig. 1, with the differences that we consider the systematic bias in the dimensionless spin on the BH here, and that the differences shown are absolute and not fractions of the injected spin. In the bottom row, we show a control run where both injected and template waveforms correspond to binary black holes.

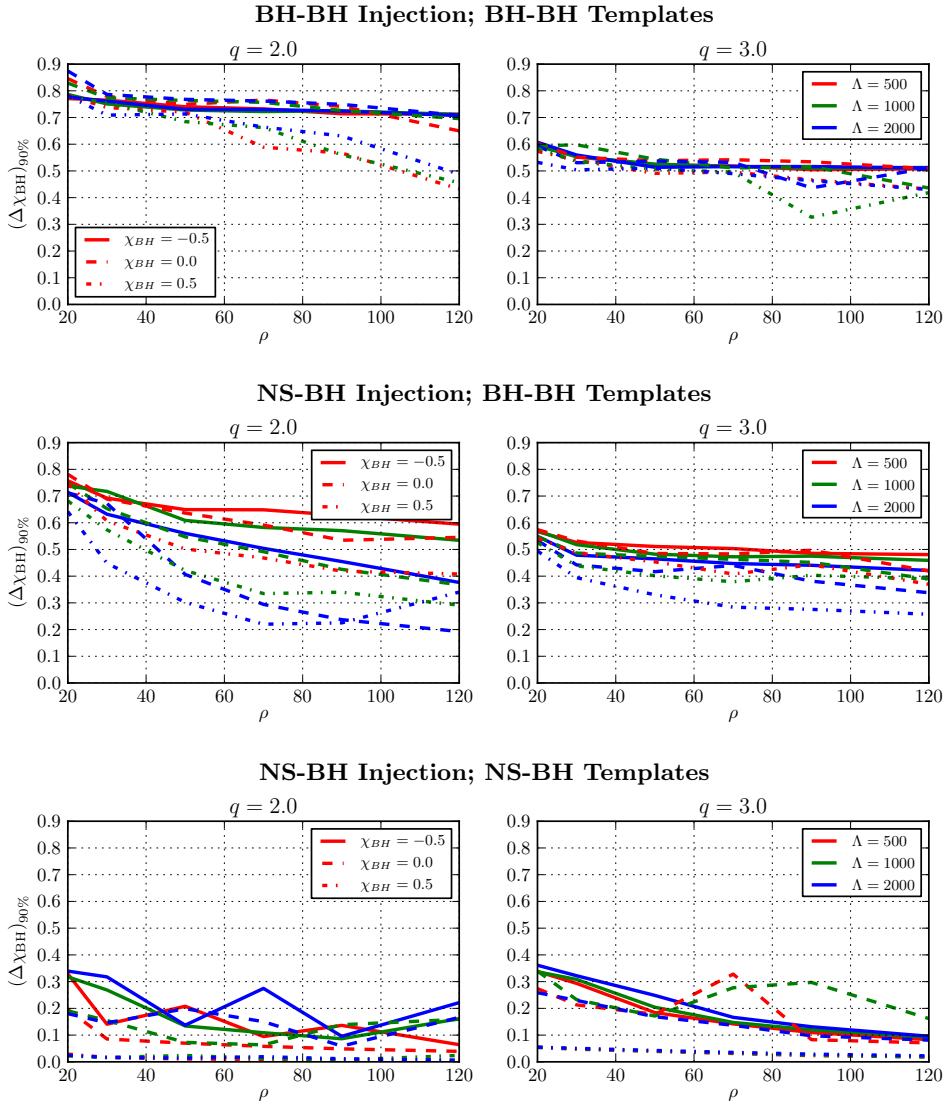

FIG. 6. The top two rows in the figure are similar to Fig. 2, with the difference that we consider the confidence intervals in the recovery of the dimensionless spin on the BH $\chi_{\rm BH}$ here. As in Fig. 5, we show here the absolute width of the confidence interval without normalizing with the injected spin. The bottom row show a control run where matter effects are ignored both in the injected signal and the template waveforms.

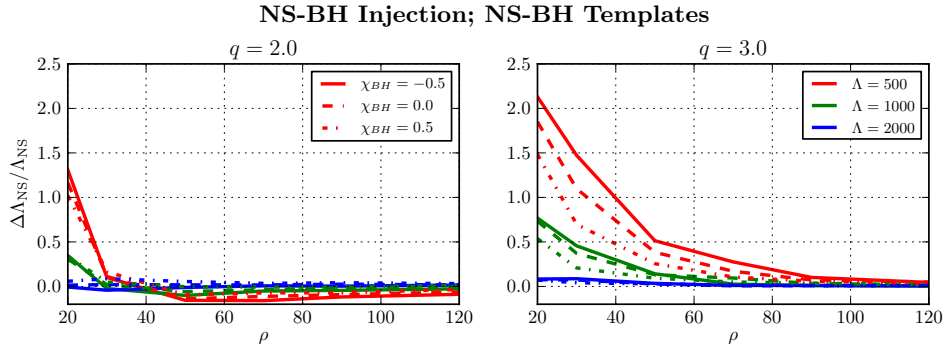

FIG. 7. This figure is similar to the bottom row of Fig. 1, with the difference that we consider the NS tidal parameter Λ here.

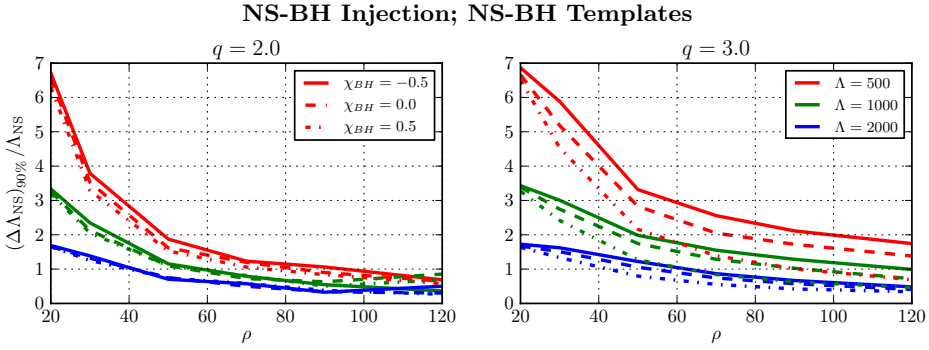

FIG. 8. This figure is similar to the bottom row of Fig. 2, with the difference that we consider the NS tidal parameter Λ here.